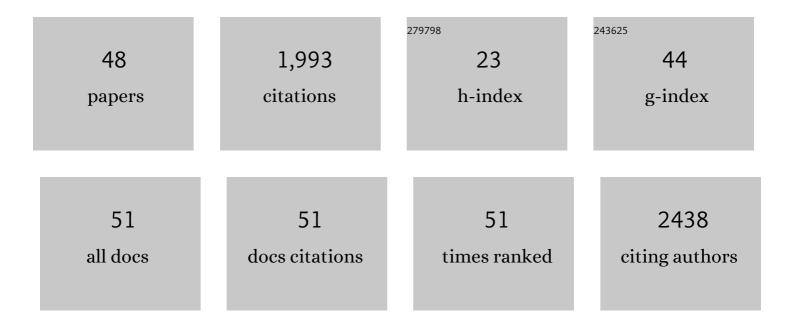
## **Uwe Wolfram**

List of Publications by Year in descending order

Source: https://exaly.com/author-pdf/7692648/publications.pdf Version: 2024-02-01



I WE WOLEDAM

#	Article	lF	CITATIONS
1	Effect of patient inhalation profile and airway structure on drug deposition in image-based models with particle-particle interactions. International Journal of Pharmaceutics, 2022, 612, 121321.	5.2	9
2	Multiscale mechanical consequences of ocean acidification for cold-water corals. Scientific Reports, 2022, 12, 8052.	3.3	6
3	Nonlinear micro finite element models based on digital volume correlation measurements predict early microdamage in newly formed bone. Journal of the Mechanical Behavior of Biomedical Materials, 2022, 132, 105303.	3.1	10
4	Heat impact during laser ablation extraction of mineralised tissue micropillars. Scientific Reports, 2021, 11, 11007.	3.3	7
5	An experimentally informed statistical elasto-plastic mineralised collagen fibre model at the micrometre and nanometre lengthscale. Scientific Reports, 2021, 11, 15539.	3.3	8
6	Extrafibrillar matrix yield stress and failure envelopes for mineralised collagen fibril arrays. Journal of the Mechanical Behavior of Biomedical Materials, 2020, 105, 103563.	3.1	5
7	Crumbling Reefs and Cold-Water Coral Habitat Loss in a Future Ocean: Evidence of "Coralporosis―as an Indicator of Habitat Integrity. Frontiers in Marine Science, 2020, 7, .	2.5	36
8	Compressive behaviour of uniaxially aligned individual mineralised collagen fibres at the micro- and nanoscale. Acta Biomaterialia, 2019, 89, 313-329.	8.3	36
9	Compositional and mechanical properties of growing cortical bone tissue: a study of the human fibula. Scientific Reports, 2019, 9, 17629.	3.3	31
10	"Peroperative estimation of bone quality and primary dental implant stability― Journal of the Mechanical Behavior of Biomedical Materials, 2019, 92, 24-32.	3.1	20
11	Registration of phaseâ€contrast images in propagationâ€based Xâ€ray phase tomography. Journal of Microscopy, 2018, 269, 36-47.	1.8	7
12	Comparative Analysis of Bone Structural Parameters Reveals Subchondral Cortical Plate Resorption and Increased Trabecular Bone Remodeling in Human Facet Joint Osteoarthritis. International Journal of Molecular Sciences, 2018, 19, 845.	4.1	11
13	A new multiscale micromechanical model of vertebral trabecular bones. Biomechanics and Modeling in Mechanobiology, 2017, 16, 933-946.	2.8	13
14	Nanoscale deformation mechanisms and yield properties of hydrated bone extracellular matrix. Acta Biomaterialia, 2017, 60, 302-314.	8.3	58
15	A rate-independent continuum model for bone tissue with interaction of compressive and tensile micro-damage. Journal of the Mechanical Behavior of Biomedical Materials, 2017, 74, 448-462.	3.1	3
16	Response to the commentary on mechanical properties of cortical bone and their relationships with age, gender, composition and microindentation properties in the elderly. Bone, 2017, 105, 312-314.	2.9	5
17	Post-yield and failure properties of cortical bone. BoneKEy Reports, 2016, 5, 829.	2.7	63
18	European Society of Biomechanics S.M. Perren Award 2016: A statistical damage model for bone tissue based on distinct compressive and tensile cracks. Journal of Biomechanics, 2016, 49, 3616-3625.	2.1	11

Uwe Wolfram

#	Article	IF	CITATIONS
19	Mechanical properties of cortical bone and their relationships with age, gender, composition and microindentation properties in the elderly. Bone, 2016, 93, 196-211.	2.9	207
20	Characterizing microcrack orientation distribution functions in osteonal bone samples. Journal of Microscopy, 2016, 264, 268-281.	1.8	26
21	Structural Behavior of Human Lumbar Intervertebral Disc under Direct Shear. Journal of Applied Biomaterials and Functional Materials, 2015, 13, 66-71.	1.6	9
22	Continuum damage interactions between tension and compression in osteonal bone. Journal of the Mechanical Behavior of Biomedical Materials, 2015, 49, 355-369.	3.1	36
23	Axial knee alignment influences the repair of focal articular cartilage defects – A translational study in sheep. Osteoarthritis and Cartilage, 2015, 23, A143-A144.	1.3	0
24	Particle tracking during Ostwald ripening using time-resolved laboratory X-ray microtomography. Materials Characterization, 2014, 90, 185-195.	4.4	26
25	Validation of composite finite elements efficiently simulating elasticity of trabecular bone. Computer Methods in Biomechanics and Biomedical Engineering, 2014, 17, 652-660.	1.6	3
26	In situ micropillar compression reveals superior strength and ductility but an absence ofÂdamage inÂlamellar bone. Nature Materials, 2014, 13, 740-747.	27.5	154
27	A generalized anisotropic quadric yield criterion and its application to bone tissue at multiple length scales. Biomechanics and Modeling in Mechanobiology, 2013, 12, 1155-1168.	2.8	58
28	Identification of a crushable foam material model and application to strength and damage prediction of human femur and vertebral body. Journal of the Mechanical Behavior of Biomedical Materials, 2013, 26, 136-147.	3.1	12
29	Measurement of structural anisotropy in femoral trabecular bone using clinical-resolution CT images. Journal of Biomechanics, 2013, 46, 2659-2666.	2.1	34
30	Effect of Subchondral Drilling on the Microarchitecture of Subchondral Bone. American Journal of Sports Medicine, 2012, 40, 828-836.	4.2	109
31	Hydrogels for nucleus replacement—Facing the biomechanical challenge. Journal of the Mechanical Behavior of Biomedical Materials, 2012, 14, 67-77.	3.1	51
32	Fabric-based Tsai–Wu yield criteria for vertebral trabecular bone in stress and strain space. Journal of the Mechanical Behavior of Biomedical Materials, 2012, 15, 218-228.	3.1	66
33	Internal morphology of human facet joints: comparing cervical and lumbar spine with regard to age, gender and the vertebral core. Journal of Anatomy, 2012, 220, 233-241.	1.5	17
34	Impact of measurement errors on the determination of the linear modulus of human meniscal attachments. Journal of the Mechanical Behavior of Biomedical Materials, 2012, 10, 120-127.	3.1	5
35	Highâ€resolution ZTE imaging of human teeth. NMR in Biomedicine, 2012, 25, 1144-1151.	2.8	109
36	Autofluorescence imaging, an excellent tool for comparative morphology. Journal of Microscopy, 2011, 244, 259-272.	1.8	95

3

Uwe Wolfram

#	Article	IF	CITATIONS
37	In vivo degradation of low temperature calcium and magnesium phosphate ceramics in a heterotopic model. Acta Biomaterialia, 2011, 7, 3469-3475.	8.3	119
38	Damage accumulation in vertebral trabecular bone depends on loading mode and direction. Journal of Biomechanics, 2011, 44, 1164-1169.	2.1	59
39	Valid μ finite element models of vertebral trabecular bone can be obtained using tissue properties measured with nanoindentation under wet conditions. Journal of Biomechanics, 2010, 43, 1731-1737.	2.1	83
40	Internal forces and moments in the femur of the rat during gait. Journal of Biomechanics, 2010, 43, 2473-2479.	2.1	53
41	TRANSVERSE ISOTROPIC ELASTIC PROPERTIES OF VERTEBRAL TRABECULAR BONE MATRIX MEASURED USING MICROINDENTATION UNDER DRY CONDITIONS (EFFECTS OF AGE, GENDER, AND VERTEBRAL LEVEL). Journal of Mechanics in Medicine and Biology, 2010, 10, 139-150.	0.7	13
42	Rehydration of vertebral trabecular bone: Influences on its anisotropy, its stiffness and the indentation work with a view to age, gender and vertebral level. Bone, 2010, 46, 348-354.	2.9	112
43	Correspondences of hydrostatic pressure in periodontal ligament with regions of root resorption: A clinical and a finite element study of the same human teeth. Computer Methods and Programs in Biomedicine, 2009, 93, 155-161.	4.7	53
44	A downloadable meshed human canine tooth model with PDL and bone for finite element simulations. Dental Materials, 2009, 25, e57-e62.	3.5	15
45	Vertebral trabecular main direction can be determined from clinical CT datasets using the gradient structure tensor and not the inertia tensor—A case study. Journal of Biomechanics, 2009, 42, 1390-1396.	2.1	17
46	Statistical osteoporosis models using composite finite elements: A parameter study. Journal of Biomechanics, 2009, 42, 2205-2209.	2.1	7
47	A method to obtain surface strains of soft tissues using a laser scanning device. Journal of Biomechanics, 2008, 41, 2402-2410.	2.1	17
48	Periodontal Ligament Hydrostatic Pressure with Areas of Root Resorption after Application of a Continuous Torque Moment. Angle Orthodontist, 2007, 77, 653-659.	2.4	84